Journal of Engineering Science and Technology
20th EURECA 2023 Special Issue October (2024) 107 - 121

DESIGN AN ADJUSTABLE ANKLE CONTROLLER WITH ANKLE-FOOT ORTHOSIS FOR FOOT DROP PATIENTS

P. X. KU*, W. H. ONG

School of Engineering, Digital Health and Medical Advancement Impact Lab, Taylor's University, Taylor's Lakeside Campus, No. 1 Jalan Taylor's, 47500, Subang Jaya, Selangor DE, Malaysia
*Corresponding Author: peixuan.ku@taylors.edu.my

Abstract

Ankle-foot orthosis is a device that straps onto the shin and foot of the user who experiences foot drop to ensure that the ankle and foot are locked in place. The project aimed to create the design of an ankle-foot orthosis to enable plantarflexion resistance to strengthen the dorsiflexor and plantarflexor muscle group by altering the angle between the shin and foot using the adjustable ankle controller. The computer-aided design for the ankle-foot orthosis with an adjustable ankle controller was modelled using SolidWorks software. The design model was analysed to obtain deformation, total stress and factor of safety using a static structural of analysis system. The prototype was fabricated using 3D printing with acrylonitrile butadiene styrene for rapid prototyping. The coding for the electrical components was completed using Arduino IDE software. The simulation was conducted using finite element analysis with static structural analysis to analyse the total deformation, equivalent strain, and safety factor. The functionality test was conducted by measuring varying plantarflexion angles of the adjustable ankle controller and the redundancy test was to ensure that all the mechanical components and coding were within proper operating order. An electromyography analysis on the activation of dorsiflexor muscle group was conducted in the controlled seat and walking condition. The tibialis anterior achieves a higher muscle activation signal at 0.001945545V during the walking with adjustable ankle controller test. The current study demonstrates that the adjustable ankle controller could effectively increase the rehabilitation of the dorsiflexor muscle group which will strengthen the dorsiflexor muscle group. It may provide a long-term passive recovery solution for foot drop patients.

Keywords: AFO, Arduino, Electromyography, Finite element analysis, Movement controller.

1. Introduction

The adjustable ankle controller with an ankle-foot orthosis (AFO) is a revolutionary rehabilitative device that will strengthen the dorsiflexor muscle groups by altering the plantarflexion angle whilst immobilising the ankle and acting as a solution for foot drop patients. The variable ankle locking mechanism will ensure activation and strengthening of dorsiflexor muscle groups which will solve foot drop by alleviating toe drag and achieving proper plantarflexion. Different-sized calf would achieve proper fitment by utilising a compression mechanism system.

Walking and standing rely on the ankle's primary motions: dorsiflexion and plantarflexion. These motions have a limited angle range from the neutral position in the coronal plane, typically around 30° [1]. An individual's daily activities, such as sports or achieving a minimum step count, can expand this range due to the strengthening of dorsiflexor muscle groups and the extension of tendons and ligaments [2]. Human flexibility tends to decrease during growth as tendons and ligaments solidify, but the range of motion in normal activities varies. For example, during walking, it's about 30°, while ascending stairs allows for 37°, and descending stairs permits up to 56° [3]. The standard walking gait follows a cyclical pattern, involving the heel rocker, ankle rocker, and foot rocker phases. The heel rocker starts when the heel touches the ground, marking the return of the foot to a neutral position. The ankle rocker phase occurs as the foot transitions from plantarflexion to dorsiflexion, causing the shank (tibia and fibula) to pivot forward. Finally, during the foot rocker phase, the heel lifts off, reaching a maximum plantarflexion of 14° [4], while power generation at the toe-off stage for walking takes place. Furthermore, the study indicates that a static load of 1.5kN on the lower extremities results in a pressure reading of 9.9MPa across a specific area [5]. This finding underscores the importance of carefully considering all forces generated during the AFO design process to ensure its durability and long-term performance.

Patients dealing with foot drop have options for passive recovery, including physical therapy and ankle braces [6]. Physical therapy, guided by a skilled physiotherapist, involves targeted exercises to strengthen the dorsiflexor muscle groups, which can reduce the impact of foot drop and enhance control and functionality [7]. Alternatively, supportive ankle braces offer a mechanical solution by securing the foot, minimizing unintended movements, and reducing the risk of foot drop occurrences. The treatment for foot drop comprises a mix of active and passive approaches, each with its unique benefits. Healthcare providers play a crucial role in tailoring these treatments to individual patient needs to ensure optimal outcomes and a path toward improved mobility and quality of life.

AFO selection involves two primary types: solid AFOs, with a fixed ankle angle, and dynamic AFOs, allowing adjustable plantarflexion resistance [8]. Evaluating AFO efficacy considers AFO type and its impact on gait and foot drop conditions, focusing on the shin-down region. It aims to enhance gait function and kinetics, distinguishing AFO users from non-users [8]. Assessing AFO effectiveness starts with examining gait function, including step cadence and ankle sagittal plane dynamics. AFO users exhibit a higher cadence, signifying improved foot stability and balanced walking [9]. Previous studies has shown that AFO users have a cadence 0.42 times greater than non-users, validating the advantages of AFOs in preventing foot drop at a 95% confidence [10].

The development and usage of AFO play a pivotal role in addressing medical conditions such as foot drop which may significantly impair mobility and daily activities. Foot drop, characterised by weakness of the dorsiflexor muscle groups, presents challenges for patients, particularly those recovering from conditions like stroke. Current AFO designs offer a solution by immobilising the ankle and facilitating dorsiflexion, there are notable limitations in the functionality and practicality of designs. All current AFOs are customised based on static measurements for the patients' anthropometric characteristics and it does not include the change of muscle strength or flexibility changes at the ankle of the patient. Hence, the objective of the paper is to develop an adjustable ankle controller that allows the patient to alter the plantarflexion angle based on a recommended range from medical practitioners to induce plantarflexion resistance to produce a rehabilitative recovery process of foot drop by strengthening the dorsiflexor muscle groups. This will allow the foot drop patient to constantly enhance the muscle of dorsiflexor group without having to attend specific physical therapy sessions.

2. Methods

The project focuses on creating an adjustable ankle controller and an associated AFO prototype to aid foot drop patients. The details of design simulation and assembly processes used in this study were stated.

2.1. CAD model of prototype

Using SolidWorks software, the 3D Computer Aided Design (CAD) model of the AFO was created based on the finalized designs for the adjustable ankle controller, compression mechanism, and ankle bracing. The adjustable ankle controller served as the main system, comprised of multiple integrated subsystems to ensure proper operation (Fig. 1). The completed sub systems were assembled to complete a super system which is the adjustable ankle controller with AFO.

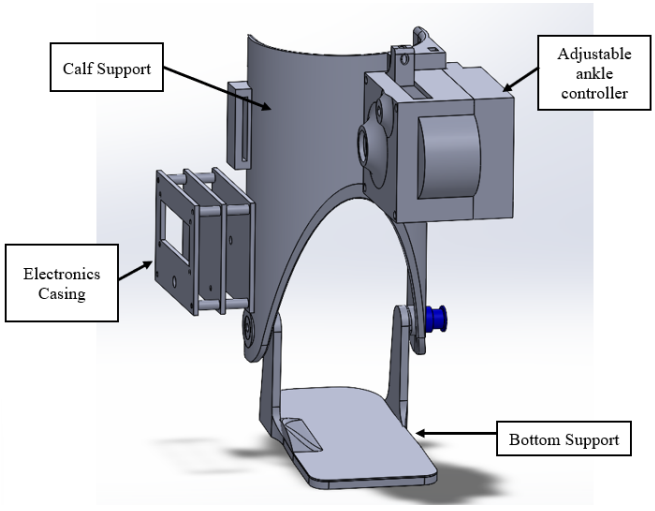

Fig. 1. CAD model of the prototype.

The adjustable ankle controller was designed with a straight-cut gearbox (Fig. 2), where a single driving gear controls the speed of driven gears. In this setup, an SG90 servo controlled a spur gear, which drives a gear and pulley system connected through a centre shaft. This centre shaft contained a locking gear and a driven spur gear that rotates independently on a 605ZZ bearing, ensuring smooth rotation. A GT2 20-tooth pulley was securely fixed on the centre pin with a setting pin to lock it in place. For safety, a spring compression system was used in the locking gear to secure the release arm redundantly, enhancing safety. The adjustable ankle controller was 3D printed by using PLA filament, chosen for its better layer adhesion and promotion of component tensile strength. PLA also results in a smoother outer surface on the gears, reducing friction and overall wear [11]. While Acrylonitrile Butadiene Styrene (ABS) material could be used, its rough surface would require smoothing with acetone vapour, which may alter the gear dimensions.

However, ABS was used for the centre pin due to its stiffer material properties, making it less prone to bending over extended use [12]. The casing of the adjustable ankle controller was closed securely with four M5 X10 bolts. The AFO comprised just two components: the calf support and the bottom support (Fig. 2(a)) and both were 3D printed using lightweight and flexible ABS filament [11]. ABS's flexibility is crucial for comfort, as it adapts to muscle movements while minimizing material fatigue. These supports feature a pivot point with a smooth 605ZZ bearing rotation and connect to the adjustable ankle controller via a GT2 20-tooth pulley and belt. The bottom support was placed inside the user's shoe, and it is used to regulate the plantarflexion angle.

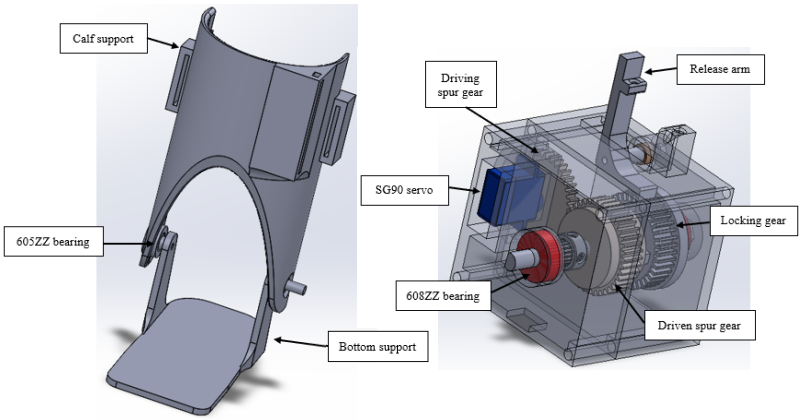

(a) AFO structure. **(b) Adjustable ankle controller.**

Fig. 2. Labelled diagram of AFO with the adjustable ankle controller system.

2.2. ANSYS simulation

Analysis system simulation software (ANSYS), with finite element analysis, was used in the current study [13]. ANSYS aids in modelling and predicting adjustable ankle controller and AFO performance, streamlining designs, reducing costs, and mitigating risks. Its significance in modern engineering for efficiency and safety. To determine the best meshing method, an analysis was conducted to determine the most suitable meshing method by comparing the tetrahedron and hexagonal

dominant meshing methods at an element size of 0.01m based on skewness as a measure of quality. A lower skewness value was used as selected as a higher skewness will produce inaccurate results. The chosen meshing method was tetrahedron as it has an overall lower skewness value at 0.51189 whereas the hexagonal dominant method is 0.6955, as lower skewness value will produce a higher accuracy simulation. A mesh size of 0.006m was chosen due to its minimal percentage difference and accurate total deformation at 0.99001m. The difference between mesh sizes of 0.006m and 0.004m was just 0.00596%, which wouldn't significantly impact result accuracy. This choice ensures that numerical analysis provides accurate real-life results. However, hardware limitations and time constraints may influence the selection of a 0.006m mesh size. Smaller mesh sizes demand more processing power and time, which the available hardware couldn't accommodate. Therefore, balancing accuracy and hardware capability led to the decision to use a 0.006m mesh size.

Establishing proper boundary conditions, including fixed supports, and loading points, is crucial as they determine the entire simulated study and ensure a close resemblance to real-life applied forces. For the AFO, fixed supports were represented by the M3 bolt slot and the GT2 20T pulley housing, serving as pivotal connections between the calf and bottom support for static structural analysis as shown in Fig. 3(a).

This static structural analysis aims to replicate the stress and applied force during the toe-off phase of gait, where the AFO experiences the highest force of 1500N. The applied force was directed towards the inner section of the calf support, in the negative x-axis direction (Fig. 3(b)). To verify that the bottom support can withstand the weight of an average male (60kg), the weight was calculated based on the weight of the average male acting on the bottom support. Eq. (1) was used for the weight calculation based on International Standard Operation 80000-4:2019 [14] is:

$$Weight = Mass \times Gravitational \quad (1)$$

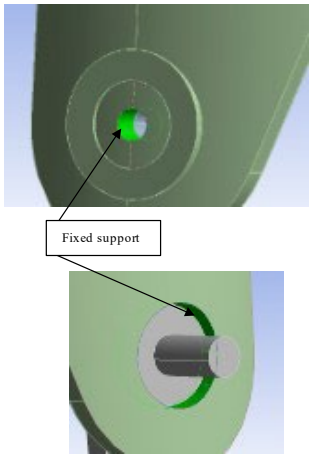

(a) Fixed support on M3 bolt slot (above) and GT2 pulley housing (below).

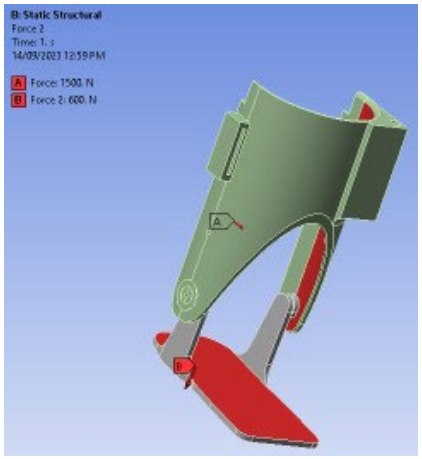

(b) Applied force on AFO structure.

Fig. 3. Boundary conditions for the AFO design.

This calculation serves a critical purpose by verifying the structural integrity of the AFO's bottom support. The weight action on the person would be 558.6N when the mass of the average Asian male is 60kg. However, a weight of 600N is used to represent the weight of a person because the weight of males may fluctuate. The load-bearing capacity of the AFO's bottom support is of utmost importance as it ensures stability, comfort, and safety for the user. By conducting this calculation, engineers and designers can be confident that the AFO will effectively provide the necessary support and maintain its functionality, even when subjected to the body weight and gravitational forces of the wearer during typical daily activities. ANSYS was conducted to obtain the total deformation, equivalent strain and safety factor of the AFO structure constructed from PLA and ABS [15].

2.3. Fabrication of prototype

The 3D printing process for components involves three main steps: 3D printing prototype components, post-finishing, and dry fitting. First, the CAD files were converted into universally accepted STL files, followed by the customization of printing parameters using slicing software. These parameters, including printing speed, infill density, and support structures, are tailored to the specific filament being used. It is important to note that the adjustable ankle controller is constructed from PLA and AFO structure is constructed from ABS. Notably, PLA and ABS filaments require different settings due to their material differences. When precision is crucial, such as for components like locking gears and spur gears, slower printing speeds are employed to ensure dimensional accuracy. This precision is especially important in the production of complex medical devices like the adjustable ankle controller and AFO. For PLA filament, a nozzle temperature of 190ºC and a bed temperature of 60ºC were used, with a 70% infill density and a printing speed of 75 mm/s [16].

In contrast, ABS filament required a higher nozzle temperature of 210ºC, a bed temperature of 100ºC, 100% infill density, and a printing speed of 60 mm/s [17]. Layer height remains constant at 0.25 mm. These differences emphasize the importance of selecting appropriate printing parameters based on the filament type to achieve optimal results. The choice of infill density is a critical decision, balancing flexibility, and tensile strength, and it affects material weight and costs. Higher infill densities result in increased weight and expenses, necessitating a trade-off in the production of AFO and the adjustable ankle controller.

The second step involved the actual 3D printing of components using a specific printer, the Raise 3D Pro Plus. The G-code generated from the slicing software was uploaded into the printer, and printing occurs within an enclosed space to maintain consistent temperature conditions, ensuring better layer adhesion and reducing the risk of air bubbles. After printing, components slowly cooled in the enclosure to prevent temperature-induced cracks. Both PLA and ABS filaments were dehydrated before use to prevent nozzle clogs and reduce stringing issues. Dry fitting is crucial to ensure proper fitment, as 3D-printed components may change dimensions due to post-printing shrinkage. Any excess burrs from support structures were sanded down to ensure precise fitment. Quality checks were performed on all components to identify defects, and any flawed pieces were reprinted.

2.4. Electronic assembly

The electronics for the adjustable ankle controller were centred around an Arduino Uno microcontroller due to its open-source nature, enabling cost-effective software development with readily available libraries and tools. The liquid crystal library is already accessible within Arduino IDE for the controller's liquid crystal display (LCD) to show the plantarflexion angle. A 500kΩ potentiometer acts as the analogy signal controller, allowing users to adjust the angle precisely. An SG90s servo motor with metal gearing was used to ensure durability and achieve the required 15º plantarflexion angle. A physical locking mechanism in the controller was used to eliminate the need for the servo to resist gear movement during gait.

2.5. Prototype assembly

The assembly of the adjustable ankle controller, AFO, and electronic casing follows a sequential process. Initially, the parts are assembled separately and connected via mounting points on the calf support. The adjustable ankle controller was first assembled, featuring two press-fit 608ZZ bearings for stability, followed by the other half of its casing houses, 608ZZ bearing, locking mechanism, and the centre pin, which also hosts the locking gear and driven spur gear. The centre pin has a keyed shaft to prevent the gear slipping under torque. A GT2 20 teeth pulley was attached to the driven spur gear.

Both halves of the adjustable ankle controller housing were secured together with four M5 X 6cm bolts, creating an enclosure. Silicon grease was injected into the centre pin's end cap to reduce frictional wear and prevent rust, ensuring smooth rotation. The adjustable ankle controller was mounted onto the slotted inserts of the calf support, allowing users to adjust the GT2 belt tension using M5 nuts within the provided slots. This feature eliminates the need to send the entire AFO back for belt tension adjustments.

The calf support was connected to the bottom support through a 605ZZ bearing at the pivot point, with a thread locker added to the bolt threads to enhance stability. Another GT2 20 teeth pulley was secured to the bottom support using locking pins. This assembly process ensures the proper functioning and adjustability of the ankle controller and AFO components. The overall dimensions of the prototype would be 0.18 m × 0.20 m × 0.25 m (Fig. 4).

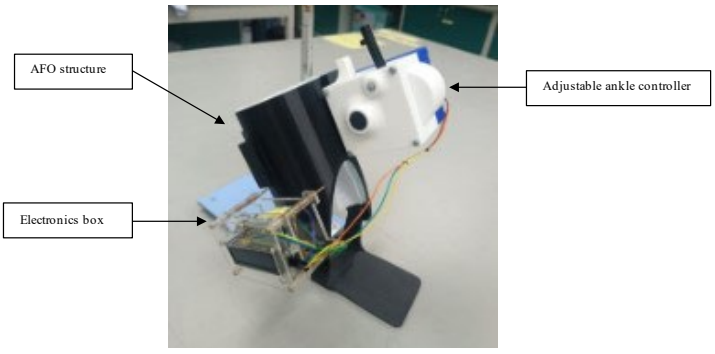

Fig. 4. Prototype of completed adjustable ankle controller, electronics box and AFO.

2.6. Functionality test

The functionality test was conducted for the first week of continuous usage by using a goniometer to measure the angle between the sole of the bottom support and the outer surface of the calf support. The AFO structure with an adjustable ankle controller was prepared by switching on the power to the electronics box and the potentiometer was adjusted until a plantarflexion angle of 5º, 10º, 15º and 20º. The reference point of the goniometer was set to zero. Then the goniometer's stationary arm was aligned with the surface of the neutral, and the moving arm was placed on the sole of the bottom support. The goniometer was zeroed to ensure that if zero error is present then it would be accounted for during the measurement of the plantarflexion angle. The plantarflexion angle was measured five times, and the measurement would be average to prevent any error from affecting the accuracy of the data collection. To determine that the servo stepping accuracy of the adjustable ankle controller, and the tension of the belt is maintained throughout the usage of one month, the functionality test was repeated after a month.

2.7. Electromyography test

Electromyography (EMG) is a diagnostic test that measures the electrical activity in the dorsiflexor muscle group, responsible for lifting the foot and toes during dorsiflexion [18]. In this study, the EMG assessed the tibialis anterior, extensor digitarum longus, and extensor hallucis longus muscles under normal conditions with the use of an adjustable ankle controller and AFO (Fig. 5). The Delsys Trigno Wireless System was employed, utilizing three wireless modules to monitor electrical signals from the dorsiflexor muscles. Before applying these modules to test subjects, the application area was meticulously cleaned with alcohol swabs to ensure a clean contact surface between the modules and the skin. The wireless modules were mapped to each muscle using Delsys Acquisition software and placed on the skin over the dorsiflexor muscle groups. Data was collected during the EMG examination by the same software to generate graphical representations of the data.

Fig. 5. Application of wireless module on lower limb of the test subject.

Once the location of the wireless module was confirmed, the EMG test was conducted. There are a total of four conditions that would be simulated with 10 of the

test subjects. The first test required the test subject to sit down on a chair and relax the ankle, this determined if the dorsiflexor muscles are activated during resting.

The second test required the test subject to sit down on a chair and relax the ankle while wearing the adjustable ankle controller with AFO at a plantarflexion angle of 10º to determine if the dorsiflexor muscles are activated whilst using the adjustable ankle controller with AFO. The first and second tests were simulated the test subjects resting while conducting their daily activities and if the adjustable ankle controller will promote rehabilitative strengthening of the dorsiflexor muscle groups.

The third test required the test subject to walk for 15s in a straight line on a flat surface to determine the muscle activation of dorsiflexor muscle group and the fourth test required the test subject to walk for 15s in a straight line on a flat surface with the adjustable ankle controller with AFO at plantarflexion angle of 10º to determine if there is an increase of muscle activation of the dorsiflexor muscle group.

2.8. Data Analysis

The raw data obtained from the EMG results would filter infinite impulse response to determine the 0 points of the test and to conduct time-frequency analysis using the Delsys Acquisition software. The Delsys Acquisition software would filter out the infinite impulse response which is an analogue filter that enables feedback loops and removes unwanted noise within the raw data. Root mean square is applied on the filtered raw data to normalise the signals with constant magnification and removes cancellation of signals to show the actual amplitude of the raw data signal. Once the root mean square was calculated, the raw data was exported in a Microsoft Excel file which graphs were constructed to visualise the EMG results. Graphical analysis is conducted on the graphs to extract out the maximum and minimum muscle activation for the tibialis anterior, extensor digitarum longus and extensor hallucis longus for both the seated and walking conditions.

3. Result and Discussion

3.1. ANSYS simulation analysis

The most suitable material would be determined based on the three key findings (total deformation, equivalent strain, and safety factor) because it has been selected as the important criteria that the AFO structure must achieve to ensure the user is able to operate the AFO structure without any mechanical risk, ensured durability of the material utilised due to material fatigue and safety of the user. Static structural analysis was carried out on two components which are the calf support and bottom support, the data obtained is displayed in Fig. 6.

Figure 6(a) reveals that the maximum deformation, measuring 0.049446 m, occurs at the tip of the bottom support. This deformation primarily results from the continuous force exerted by the user's weight. Notably, this tip is the furthest point from the applied load, which leads to the multiplication of forces due to torque vector [18]. The calf support experiences a maximum total deformation of 0.03294 m at the top right, primarily due to the concentrated load imposed by the compression mechanism strap as shown in Fig. 6(b).

The primary cause of this localized deformation is the concentrated loading. The highest equivalent strain of 0.25451 within the AFO structure is observed at

the pillar of the bottom structure and the housing of the 605ZZ bearing. These components are essential for withstanding the dynamic movements and vibrations generated during the gait cycle.

Maintaining their equivalent strain within the limits of the ABS material is crucial to avoid material failure, including structural damage, distortion, or catastrophic breakdown that could make the device unreliable and unsafe for users [19]. A higher equivalent strain suggests that the delamination of layers will not occur within a short period due to the low elastic strain acting on the bearing housing [20]. While the majority of the AFO structure maintains a safety factor of 15, ensuring durability and user safety, certain areas exhibit lower safety ratings, with a minimum of 0.071928 experienced at the pillar of the bottom housing and the 605ZZ bearing housing (Fig. 6(c)).

Kubasad et al. [21] found that the average safety factor of 3.14 in the AFO structure design can withstand the loading conditions of normal gait comparatively to the designed AFO it has a minimum safety factor of 0.071928 which is lower than the stated safety factor at the GT2 mounting of the bottom support. This can be alleviated with heat treating the bottom support because the heat-treated parts will increase Young's modulus by 22.1% and increase overall strength by 41.1% [22], thus ensuring that the safety factor would increase.

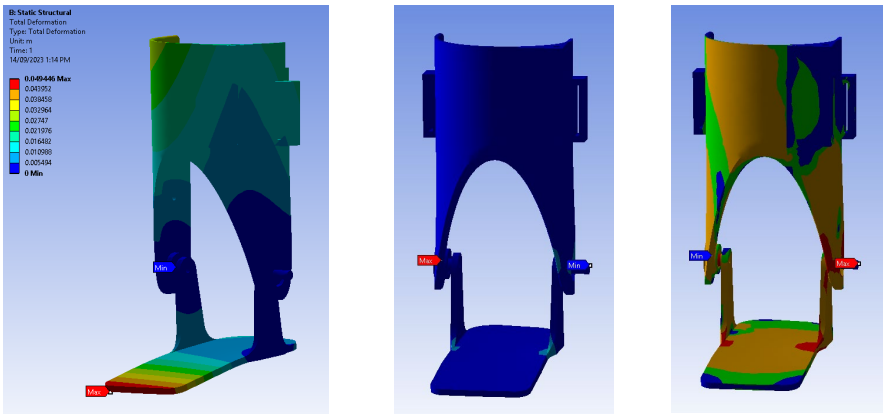

(a) Total deformation. (b) Equivalent elastic strain. (c) Safety factor.

Fig. 6. Finite element analysis on AFO structure constructed using ABS.

3.2. Functionality analysis

The average result of the functionality test of the AFO with an adjustable ankle controller that determines the accuracy of the adjustable ankle controller in manipulating the plantarflexion angle (Table 1). The adjustable ankle controller will heavily impact the functionality of the entire prototype because it is the key factor for this design to induce plantarflexion resistance, and the power and tension loss within a belt-driven system is common [23]. Fuetterer and Schlamadinger [24] also stated that tension in ribbed v-belts would be lost over some time when constant load is applied to the belting system. When tension is lost in a belting system, it would cause the driven angle to be altered and affect the functionality of the adjustable ankle controller.

Table 1. Goniometer reading for the functionality test.

Predicted plantarflexion angle (º)	Measured plantarflexion angle after 1 week usage (º)	Measured plantarflexion angle after 1 month usage (º)
5	5.00	5.33
10	10.33	10.50
15	15.33	15.33
20	20.00	20.33

Based on Table 1, shows that there are no major discrepancies between the predicted and actual plantarflexion angle because the belting system has not lost tension within the first week of constant applied load. This depicts that there is no tension lost within the belting system and it maintains the functionality of the adjustable ankle controller by accurately altering the plantarflexion angle. The tension loss shown in the findings may suggest that the belting system will lose tension as the layers and ribs of the belt are subjected to tension over a long period of time [25]. Bishe et al. [26] suggested that in an ankle controller that would require the user to utilise during gait, the accuracy of the plantarflexion angle must be kept within a 0.5º tolerance to ensure the functionality of rehabilitation of the dorsiflexor muscle group due to induced plantarflexion resistance.

3.3. Electromyography analysis

EMG results for subjects simulating with and without the adjustable ankle controller in the seated and walking conditions, both are presented in Table 2.

Table 2. EMG results for muscle activation with and with adjustable ankle controller during the seated condition and walking condition.

Condition simulated	Seated condition		Walking condition	
	With AAC	**Without AAC**	**With AAC**	**Without AAC**
Tibialis anterior				
Minimum (V)	1.10754E-50	1.90289E-52	6.83807E-48	3.92293E-39
Maximum (V)	0.000146777	6.11181E-06	0.000193561	0.000194554
Extensor digitarum longus				
Minimum (V)	2.0261E-51	3.8342E-53	2.9157E-39	6.29255E-48
Maximum (V)	9.24045E-05	5.27714E-06	9.31932E-05	8.5337E-05
Extensor hallucis longus				
Minimum (V)	7.04011E-51	5.61157E-52	8.15439E-39	7.19195E-48
Maximum (V)	8.5743E-05	5.00893E-06	0.000139683	0.000112165

* *AAC: Adjustable ankle controller*

The EMG test conducted with the subjects in a seated position, reveals that the neuromuscular system constantly engages in micro-movements to ensure ankle and foot stability [27]. These movements could triggered by subconscious actions or be influenced by ligamentous laxity, leading to subtle shifts and micro wobbles in joints that require the dorsiflexor muscles to stabilize them [28]. The plantarflexion angle that would be subjected has a range of 5º to 20º similar to the findings of Kobayashi et al. [29]. This study shows that a plantarflexion angle of 10º is sufficient to provide the required plantarflexion resistance.

The findings show that in a seated position the muscle activation of the dorsiflexor muscle group is higher with the usage of the adjustable ankle controller. The tibialis

anterior has 95% more muscle activation, extensor digitarum longus has 92.29% more muscle activation and extensor hallucis longus has 94.16% with the adjustable ankle controller. These findings suggest that the dorsiflexor muscle group experiences higher activation in the seated position with the adjustable ankle controller at plantarflexion angle of 10º [30]. Léger et al. [31] have also stated that in the seated position, active seating which is micromovements of the lower muscle is present and occurs unconsciously. The micromovements would occur to ensure the stability of the joints is retained and enhanced with the induction of plantarflexion resistance.

Besides, test subjects who utilize the adjustable ankle controller exhibit higher muscle activation, both in terms of maximum and minimum EMG signal results. In the walking with adjustable ankle controller condition, test subjects demonstrate maximum muscle activation in the tibialis anterior at 0.000193561V, extensor digitorum longus at 9.31932E-05, and extensor hallucis longus at 0.000139683V. In comparison, the test subjects in the walking without adjustable ankle controller condition exhibit maximum muscle activation in the tibialis anterior at 0.000194554V, extensor digitorum longus at 8.5337E-05, and extensor hallucis longus at 0.000112165V. It is concluded that the adjustable ankle controller will increase the dorsiflexor muscle controller during walking because the additional plantarflexion angle of 10º will cause the test subject to exert more force during the toe-off and heel strike stage as stated by Kobayashi et al. [30]. The author also suggested that a higher peak ankle power generation will increase with the subjected plantarflexion resistance due to the toe-off stage which will generate more muscle strengthening as the dorsiflexor muscle group is required to produce high peak power. This is because more force would be required to depress the heel and lift the toes when the ankle is forced to a plantarflexion angle of 10º [32]. At the same time, more force is required to push off the ball of the foot during toe-off the maintain ankle stability by contracting the dorsiflexor muscle group.

Several limitations have been encountered during the investigation of muscle activation and functionality of the adjustable ankle controller. The primary limitation arises from the project's design tailored to Asian anatomy, which differs significantly from Western anatomy, particularly in feet, calf, and ankles. This is because Asians have a different musculoskeletal size when compared to Western counterparts and the dimensions of the prototype would be different to accommodate for the different sizes. The project aims to create an AFO with an adjustable ankle controller specifically for the Asian market, considering these differences. This limitation impacts the size and design of the AFO components, as well as the choice of a servo model with lower torque to match the smaller muscle size in Asian ankles. Another limitation pertains to numerical analysis performed using ANSYS due to hardware limitations such as the processing capabilities of the computer, the meshing size is limited. The simulated results do not consider the effects of moisture that is absorbed into the PLA and ABS filament which will alter the tensile properties of the said materials.

4. Conclusions

In conclusion, this research has successfully developed an adjustable ankle controller in conjunction with an AFO to address the specific objectives of providing plantarflexion resistance as a rehabilitative therapy for individuals with foot drop. The AFO structure used ABS for its high ductility and tensile strength with the ability to conduct heat treatment to further increase its tensile strength. The adjustable ankle

controller would be driven by a servo that uses Arduino Uno to act as the control unit. The prototype enables precise control of the plantarflexion angle using a GT2 timing belt and pulley system. The findings show that it can be determined that the AFO structure would be able to withstand the applied load with a maximum deformation of 0.04944m, equivalent strain of 0.25451 and safety factor 15.

The functionality test also concludes that the adjustable ankle controller can ensure proper functionality and maintain tension in the belt system after a month of continuous applied load, and it is within the acceptable tolerance of 0.5º. Hence, maintaining the adjustable ankle controller's performance and the belt tensioning would be able to be adjusted by altering the position of the adjustable ankle controller mounting. Users who use the adjustable ankle controller during seated and walking conditions have a higher muscle activation for the dorsiflexor muscle group. All the dorsiflexor muscle groups have an average 90% increase in muscle activation during seated and walking conditions. This proves that the adjustable ankle controller may induce plantarflexion resistance and could be further applied to foot drop patients. This prototype lays the groundwork for future AFOs with integrated adjustable ankle controllers, promoting good health and well-being in line with the United Nations's third sustainable development goal. It provides a passive recovery solution for individuals with foot drop, enhancing their overall well-being and health.

Abbreviations

ABS	Acrylonitrile Butadiene Styrene
AFO	Ankle-Foot Orthosis
ANSYS	Analysis System
CAD	Computer-Aided Design
EMG	Electromyography
PLA	Polylactic Acid

References

1. Calhoun, J.H.; Li, F.; Ledbetter, B.R.; and Viegas, S.F. (1994). A comprehensive study of pressure distribution in the ankle joint with inversion and eversion. *Foot & Ankle International*, 15(3), 125-133.
2. Ku, P.X.; Osman, N.A.A.; and Abas, W.A.B.W. (2016). The limits of stability and muscle activity in middle-aged adults during static and dynamic stance. *Journal of Biomechanics,* 49(16), 3943-3948.
3. Nordin, M.; and Frankel, V.H. (2001). *Basic biomechanics of the musculoskeletal system*. Lippincott Williams & Wilkins.
4. Vasiliauskaite, E. et al. (2021). A study on the efficacy of AFO stiffness prescriptions. *Disability and Rehabilitation: Assistive Technology,* 16(1), 27-39.
5. Pirker, W.; and Katzenschlager, R. (2017). Gait disorders in adults and the elderly : A clinical guide. *Wiener Klinische Wochenschrift*, 129(3), 81-95.
6. van Swigchem, R.; van Duijnhoven, H.J.R.; den Boer, J.; Geurts, A.C.; and Weerdesteyn, V. (2012). Effect of peroneal electrical stimulation versus an ankle-foot orthosis on obstacle avoidance ability in people with stroke-related foot drop. *Physical Therapy,* 92(3), 398-406.

7. Kaus, J. (2011). ActiGait - A partly implantable drop foot stimulator in apoplectic stroke. *Gait & Posture,* 33, S54.
8. Gök, H.; Küçükdeveci, A.; Altinkaynak, H.; Yavuzer, G.; and Ergin, S. (2003). Effects of ankle-foot orthoses on hemiparetic gait. *Clinical Rehabilitation,* 17(2), 137-139.
9. Choo, Y.J.; and Chang, M.C. (2021). Effectiveness of an ankle-foot orthosis on walking in patients with stroke: a systematic review and meta-analysis. *Scientific Reports,* 11(1), 15879.
10. Choi, H.; and Kim, Y. (2008). Foot/ankle roll-over characteristics for different joint alignments of the Ankle-foot orthosis (AFO) during level walking. *Proceedings of the International Conference on BioMedical Engineering and Informatics*, Sanya, China, 872-874.
11. Rodríguez-Panes, A.; Claver, J.; and Camacho, A.M. (2018). The influence of manufacturing parameters on the mechanical behaviour of PLA and ABS pieces manufactured by FDM: a comparative analysis. *Materials,* 11(8), 1333.
12. Zisopol, D.G.; Nae, I.; Portoaca, A.I.; and Ramadan, I. (2022). A statistical approach of the flexural strength of PLA and ABS 3D printed parts. *Engineering*, *Technology* & *Applied Science Research*, 12(2), 8248-8252.
13. Wahab, M.A. (2014). *The mechanics of adhesives in composite and metal joints: finite element analysis with ANSYS*. DEStech Publications, Inc.
14. Newell, D.B.; and Tiesinga, E. (2019). *The international system of units (SI)*. National Institute of Standards and Technology.
15. Ali, M.H.; Smagulov, Z.; and Otepbergenov, T. (2021). Finite element analysis of the CFRP-based 3D printed ankle-foot orthosis. *Procedia Computer Science,* 179, 55-62.
16. Afonso, J.A. et al. (2021). Influence of 3D printing process parameters on the mechanical properties and mass of PLA parts and predictive models. *Rapid Prototyping Journal,* 27(3), 487-495.
17. Samykano, M. et al. (2019). Mechanical property of FDM printed ABS: influence of printing parameters. *The International Journal of Advanced Manufacturing Technology,* 102, 2779-2796.
18. Mills, K.R. (2005). The basics of electromyography. *Journal of Neurology, Neurosurgery and Psychiatry,* 76(2), 32-35.
19. Lin, W.; and Yoda, T. (2017). *Repair, strengthening, and replacement.* In Lin, W.; and Yoda, T. (Eds.), *Bridge engineering: Classifications, design loading, and analysis methods*. Butterworth-Heinemann.
20. Barile, C.; Casavola, C.; and Cazzato, A. (2018). Acoustic emissions in 3D printed parts under mode I delamination test. *Materials*, 11(9), 1760.
21. Kubasad, P.R.; Gawande, V.A.; Todeti, S.R.; Kamat, Y.D.; and Vamshi, N. (2020). Design and analysis of a passive ankle foot orthosis by using transient structural method. *Journal of Physics: Conference Series,* 1706(1), 012203.
22. Amza, C.G.; Zapciu, A.; Constantin, G.; Baciu, F.; and Vasile, M.I. (2021). Enhancing mechanical properties of polymer 3D printed parts. *Polymers,* 13(4), 562.
23. Gerbert, B.G. (1974). Power loss and optimum tensioning of V-belt drives. *Journal of Manufacturing Science and Engineering,* 96(3), 877-885.

24. Fuetterer, W.G.; and Schlamadinger, H.J. (1980). Belt tension decay of automotive V and V-ribbed belts. *SAE Technical Paper*, 800851.
25. Wilczyński, M.; and Domek, G. (2019). Influence of tension layer quality on mechanical properties of timing belts. *MATEC Web Conferences,* 254, 05010.
26. Bishe, S.S.P.A.; Nguyen, T.; Fang, Y.; and Lerner, Z.F. (2021). Adaptive ankle exoskeleton control: validation across diverse walking conditions. *IEEE Transactions on Medical Robotics and Bionics,* 3(3), 801-812.
27. Kaneda, K. (2019). The features of muscle activity during chair standing and sitting motion in submerged condition. *PLoS One,* 14(8), e0220602.
28. Kothiyal, K.; and Kayis, B. (2001). Workplace layout for seated manual handling tasks: an electromyography study. *International Journal of Industrial Ergonomics,* 27(1), 19-32.
29. Kobayashi, T. et al. (2015). The effect of changing plantarflexion resistive moment of an articulated ankle-foot orthosis on ankle and knee joint angles and moments while walking in patients post stroke. *Clinical Biomechanics,* 30(8), 775-780.
30. Kobayashi, T. et al. (2018). Effect of plantarflexion resistance of an ankle-foot orthosis on ankle and knee joint power during gait in individuals post-stroke. *Journal of Biomechanics,* 75, 176-180.
31. Léger, M.C.; Dion, C.; Albert, W.J.; and Cardoso, M.R. (2023). The biomechanical benefits of active sitting. *Ergonomics,* 66(8), 1072-1089.
32. Davis, R.B. (1997). Reflections on clinical gait analysis. *Journal of Electromyography and Kinesiology,* 7(4), 251-257.